NASA TECHNICAL NOTE

NASA TN D-4528

HIGH ENERGY PROTON DAMAGE IN SILICON SURFACE BARRIER DETECTORS

by Jag J. Singh and Emanuel Rind

Langley Research Center
Langley Station, Hampton, Va.

NATIONAL AERONAUTICS AND SPACE ADMINISTRATION • WASHINGTON, D. C. • MAY 1968

HIGH ENERGY PROTON DAMAGE IN SILICON

SURFACE BARRIER DETECTORS

By Jag J. Singh and Emanuel Rind

Langley Research Center
Langley Station, Hampton, Va.

NATIONAL AERONAUTICS AND SPACE ADMINISTRATION

CONTENTS

HIGH ENERGY PROTON DAMAGE IN SILICON
SURFACE BARRIER DETECTORS

By Jag J. Singh and Emanuel Rind
Langley Research Center

SUMMARY

The performance of a number of silicon surface barrier detectors has been studied under bombardment with 5.0-MeV, 20.0-MeV, and 40.0-MeV protons. The detectors investigated fall under three categories: (a) normal 100 microns deep, (b) normal 500 microns deep, and (c) fully depleted (dE/dx) type, 500 microns deep. Measurements made include rate of deterioration of charge collection efficiency, variation of resolving power, variation of leakage current, variation of noise level, and changes in detector capacitance as a function of the incident proton dose. From these several data, formulas giving relationships between the proton dose and the degree of detector resolving power deterioration have been developed for the normal and fully depleted type of detectors. These formulas, in cases where uniform defect distribution occurs, are of the form

$$\phi_x = ax\left(E_0/\Delta E\right)^{1/2} \exp(-b\rho)$$

where ϕ_x is the proton dose that will produce x fold degradation in the detector resolving power, a and b are constants determined by the type of detectors, E_0 is energy of the incident protons, ΔE is the energy dissipated by the incident protons in the sensitive region of the detector and ρ is the initial base material resistivity. These formulas are expected to predict correct values of ϕ_x for $0 < x < 1$. The value of $x = 1$ corresponds to a condition when the resolving power of the detector has degraded by a factor of 2. The measurements clearly establish that (1) the fully depleted detectors are more radiation damage resistant than the normal detectors, (2) the increased collecting field across the sensitive region reduces the damage sensitivity, and (3) the damage threshold of detectors made from lower resistivity materials is higher than that of those made from higher resistivity materials. In the case of dE/dx detectors, there was no convincing evidence of any difference in degradation rates when viewed from the positive or negative sides of the detectors.

INTRODUCTION

Silicon surface barrier detectors are easy to make, have very small entrance window thickness, and show excellent spectrometric response to charged particles. However, because of the lack of knowledge of the precise nature of the surface barrier, it is difficult to separate the contribution of the bulk effects from the surface effects in the deterioration of such detectors under nuclear irradiation. This makes the interpretation of the observed results rather difficult and has discouraged systematic studies of silicon surface barrier detector performance under high energy particle bombardment. It should be possible, however, to develop phenomenological formulas correlating the relevant detector parameters with the incident radiation dose that produces a certain degree of deterioration. In this approach, one does not separate the surface effects from the bulk effects but rather correlates the joint effects with the incident radiation dose. The variation in the response of surface barrier detectors has been measured as a function of the integrated dose of the incident protons at energies of 5.0 MeV, 20.0 MeV, and 40.0 MeV and the data have been used in developing such phenomenological formulas. The results of these measurements are discussed in this paper.

SYMBOLS AND ABBREVIATIONS

Cs^{137} cesium-137 radioactive source

$\dfrac{dE}{dx}$ rate of loss of energy per unit path length

$\dfrac{dE}{dx}$ detector   fully depleted detector

E_p incident proton energy

Po^{210} polonium-210 radioactive source

T_R carrier transit time

W depletion width of detector; this is the only region across which an electric field exists

ΔE energy expended by proton in sensitive region of detector

ρ initial resistivity of detector base material

τ carrier lifetime in detector base material

ϕ_x proton dose required to produce x degree of degradation of resolving power

FWHM   full width of pulse at half its maximum height

rms   root mean square

The detectors tested were obtained from four different manufacturers who are listed as sources A, B, C, and D.

EXPERIMENTAL PROCEDURE

A schematic diagram of the general experimental technique is shown in figure 1. Protons of appropriate energies were allowed to strike the detector for a time determined by the "integrated dose points" at which detector parameters were to be measured. (These dose points were determined on the basis of the considerations that (1) the detectors are expected to show appreciable damage at the stage when the number of defects produced becomes comparable to the number of donor or acceptor impurity atoms in the base material (ref. 1) and (2) at least six intermediate measurements be made before the detector shows signs of appreciable damage.) The detector parameters measured were:

    (a) Charge collection efficiency (pulse height)
    (b) Resolving power (FWHM)
    (c) Depletion width change (capacitance)
    (d) Leakage current and rms noise

The detectors tested were obtained from four leading manufacturers and were of three types:

    100 microns deep (normal)
    500 microns deep (normal)
    500 microns deep (dE/dx)

The resistivities of the base materials ranged from 1 kΩ-cm to 28 kΩ-cm and the carrier lifetimes were reported by the manufacturers to be 500 microseconds to 3000 microseconds. A low noise linear amplifier system was used for processing the detector output. The pulse shaping network in the preamplifier utilizes two integrations and one differentiation each with 1 microsecond time constant. The resultant pulse shape has a rise time of 1.5 microseconds and the decay time of 3.9 microseconds. The main amplifier has no pulse shaping. This system insured that any changes in the pulse rise

3

time associated with increase in the resistivity of base silicon will not affect the ability to measure variation in the detector response.

A Po^{210} alpha source and a Cs^{137} electron source were used to test the detector response. The use of an electron source was intended to make a uniform probing of the entire sensitive region. In the case of dE/dx detectors, measurements were made from both sides of the detectors. In the case of the test radiation entering from the negative side (gold side), the carrier electrons are expected to experience most of the collecting field whereas the holes will experience the full field in the case of the entry from the positive side (aluminum side). It was hoped that this procedure would enable any differences to be detected in capture cross section of the defects for electrons and holes. The changes in the detector noise and leakage current were measured and correlated with the variation in alpha/electron pulse heights. Variation in resistivity was determined by measuring the junction capacitance[1] with a capacitance bridge at a test frequency of 100 kc/sec. No attempt was made to quench/anneal the defects though it is probable that some photoquenching might have occurred at the end of each exposure when the interior of the target chamber was temporarily exposed to ordinary laboratory light. All measurements were carried out at room temperature.

Typical results are shown in figures 2 to 16. In figures 2 to 12, the solid lines are the best visual fits through the experimental points. In figures 2 to 6, the channel numbers represent energy. For instance, in figure 2, for a zero proton dose, the detector from source A gives a Po^{210} alpha pulse peak at channel number 601. Thus 601 channels, in this case, will equal the Po^{210} alpha energy — namely, 5.30 MeV — and one channel will equal about 8.8 keV.

EXPERIMENTAL RESULTS

Figure 2 shows a typical effect of 5.0-MeV-proton exposure on the pulse height and pulse width of the Po^{210} alpha pulses from two 100-micron-deep detectors. The base material resistivity of the detector from source A was 1.9 kΩ-cm, whereas the source B detector base material resistivity was 1.0 kΩ-cm. Figure 3 shows a typical effect of 40.0-MeV protons on the performance of two 500-micron-deep detectors. In this figure the source A detector resistivity was 9.0 kΩ-cm, whereas the resistivity of the source B detector was 5.0 kΩ-cm. Typical behavior of a fully depleted, 500-micron-deep, dE/dx detector in the field of 40.0-MeV protons is shown in figure 4. A detailed analysis of figure 4 shows the following situation:

---

[1]The capacitance is inversely proportional to the depletion width which, in turn, is proportional to the square root of base material resistivity.

Proton dose per cm^2	$\left(\dfrac{\text{Final pulse height}}{\text{Initial pulse height}}\right)_{Al}$	$\left(\dfrac{\text{Final FWHM}}{\text{Initial FWHM}}\right)_{Al}$	$\left(\dfrac{\text{Final pulse height}}{\text{Initial pulse height}}\right)_{Au}$	$\left(\dfrac{\text{Final FWHM}}{\text{Initial FWHM}}\right)_{Au}$
3.29×10^{10}	1.00	1.00	1.00	1.00
7.52×10^{10}	1.00	1.11	1.00	1.12
1.32×10^{11}	.99	1.44	.99	1.40

From this comparison, it appears that the difference in the rates of deterioration of resolving power when viewed from the negative (gold) side and the positive (aluminum) side is not significant. This tends to indicate that the defect centers created in the sensitive region of the detector do not show any preference for electrons or holes. However, it must be recognized that the electrons and holes do not see the same field configuration in their journey to the respective collecting electrodes. Figure 5 shows Cs^{137} conversion electron spectra in two 500-micron-deep detectors. The source A detector resistivity was 9.0 kΩ-cm and the carrier lifetime was 1500 microseconds. For the detector from source B, the base material resistivity was 5.0 kΩ-cm and the carrier lifetime was again reported to be 1500 microseconds. The detector from source B was considerably better than the detector from source A at zero dose. A comparison of the degradation rates of the two detectors shows that the damage caused to the source B detector by a proton dose of 1.03×10^{11}/cm^2 is of the same order as the damage caused to the source A detector by a dose of 2.2×10^{10} protons/cm^2. This difference in damaging proton dose reflects the effect of different resistivities of the base materials. The effects of defect centers set in at a lower proton dose for the Cs^{137} electron spectra as compared with the Po^{210} alpha spectra. This may be because of the following facts:

(1) The detector thickness is less than the range of 625-keV conversion electrons in silicon and, consequently, only some of the multiple-scattered electrons will deposit their full energy in the sensitive region. The number of such electrons is small and a carrier loss resulting from a smaller number of defects per unit volume becomes noticeable.

(2) Any changes in resistivity and consequent changes in the thickness of the sensitive region will not affect the alpha spectrum as much as they affect the electron spectrum.

Figure 6 shows the Cs^{137} electron spectrum from a 500-micron-deep, dE/dx detector. It is clear from a comparison of figures 5 and 6 that a much higher proton dose is required to produce damage in a fully depleted type of detector. In figures 7 and 8, the role played by the particle energy in damaging 100-micron and 500-micron-deep detectors is compared. A close examination of these figures shows that 5.0-MeV protons cause more damage than the 20.0-MeV or 40.0-MeV protons. Hence the prime damage

determining factor, as expected, is the total energy deposited by the damaging radiation inside the depletion region and its distribution. For 40.0-MeV protons, dE/dx is essentially constant throughout the sensitive region, whereas the 5.0-MeV protons will deposit more energy towards the exit end (the positive side).

One possible way to increase the useful detector life in radiation fields may be to continually increase the collecting electric field across the detector. This will increase the carrier mobility and hence reduce the carrier capture rates at the defect centers. However, this procedure has only limited application due to the high space-charge-generated leakage current which increases with the radiation damage. The usefulness of this approach in the earlier stages of radiation damage is shown in figures 9 and 10. In figure 9, the source A detector has received an integrated 5.0-MeV proton dose of $3.71 \times 10^{10}/cm^2$, whereas the source B detector has received a dose of $6.49 \times 10^{10}/cm^2$. Both detectors show a trend towards recovery of carrier collection efficiency with increasing bias. Figure 10 shows the same type of behavior in a slightly different form. Here the ordinate is proportional to the charge collection efficiency while the abscissa is a function of the detector bias. The fact that the collected charge shows bias dependence[2] indicates the existence of appreciable carrier trapping. The inverse linear relationship of the trapped charge with the applied bias in the earlier stages of bias increase tends to lend support to the trapping-in-plasma hypothesis (ref. 3). Figure 11 shows the changes in the leakage current and the rms noise as a function of the 5.0-MeV proton integrated dose to which a 100-micron-deep detector has been exposed. Obviously, both the leakage current and the rms noise change with radiation dose in the same manner.

The effect of variation in the base material resistivity resulting from radiation damage is shown in figure 12. In this figure, the capacitance of the detector has been plotted as a function of the proton dose. However, the capacitance is inversely proportional to the depletion width which, in turn, is proportional to the square root of base material resistivity. Silicon is unique among semiconductors in tending towards intrinsic conductivity with the damage. This trend has led to the suggestion that thicker depletion width detectors could be made by exposing high resistivity materials to selected types of radiation. (See discussion by O. L. Curtis on p. 133 in ref. 4.) In such cases, it is anticipated that the changes in the carrier lifetime and mobility will not precede the

---

[2]The observed dependence of pulse height on bias may appear surprising. However, in an exact treatment of transit times in semiconductor counters, one must consider the hole transit time separately from the electron transit time (ref. 2). For surface barrier counters, the hole transit time will never be independent of detector bias. It is the hole transit time which is important in determining the pulse height since for each electron arrival at the collector, a neutralizing charge will be induced in the sensitive region until a corresponding hole is collected at the front face.

beneficial effects of increased resistivity. However, figure 12 tends to cast doubts on the usefulness of this approach. The increase in the resistance is too slow compared with the rate of carrier lifetime degradation reflected in the reduced pulse height for Po^{210} alphas. The various data are summarized in tables I to III.

DISCUSSION

A great deal of literature (refs. 1 and 4 to 8) exists on the results of radiation damage to silicon solid-state detectors. However, much of the experimental data were obtained under conditions where measurement of the damage was not the prime objective. This is particularly true for surface barrier detectors where lack of knowledge of the nature of the barrier has discouraged systematic investigation of the damage. For 5- to 40-MeV protons, it is expected that most of the damage will result from defects in the bulk of the detector. On this assumption, the damage to the detector should be directly related to the ratio $\left(\dfrac{\text{Number defects/cc}}{\text{Number donor or acceptors/cc}}\right)$ and one may be able to get an approximate idea of the tolerable integrated proton doses at different proton energies (ref. 1). Since the interaction between the incident protons and silicon nuclei takes place almost entirely by coulomb scattering, one may easily calculate the total number of defects produced along the entire track by various energy protons (ref. 4). The values calculated for three proton energies are as follows:

Proton energy, MeV	Total number of defects produced per proton
5.0	160
20.0	250
40.0	370

If each defect, finally, were to behave as an acceptor or a donor, the number of incident protons that will cause significant damage to detectors of various resistivities can be calculated.[3] Figure 13 gives the donor concentration in n-type silicon for various values of bulk resistivity (ref. 5). For example, a 5 kΩ-cm, n-type silicon material has 9.4×10^{11} donor atoms/cc. A single 20.0-MeV proton incident on a 500-micron-deep detector will produce a defect concentration of 250/cm, as seen from figure 15; this will require about 4×10^9 protons/cm^2 to produce the same number of defects/cc as the number of donor atoms/cc. However, the average experimental value of the damaging dose for the 500-micron-deep detectors, made from a 5.0 kΩ-cm material, is about

---

[3]It is assumed that significant damage is produced when the number of defects produced per cc equals the initial donor or acceptor impurity concentration.

$1 \times 10^{10}/cm^2$; this suggests that only about 50 percent of the defects finally behave as donors or acceptors.

This type calculation should be considered as highly approximate since the details of the damage process and its precise effects on the detector characteristics are not easy to explain. Any explanation of the effects of defects must separate surface effects from bulk effects and consider their distribution in the forbidden energy gap. The position of these levels is expected (ref. 4) to be independent of the type of radiation that produced the vacancy-interstitial pairs and is believed to be as shown in figure 14. The various levels have different carrier capture cross sections. These defect centers are likely to affect the performance of the detectors in the following manner:

(a) They can modify the depletion width through changes in the space charge density. Figure 12, however, tends to show that the junction capacitance variation is too small to substantiate significant changes in field distribution.

(b) They can lead to changes in the energy resolution from fluctuations in the leakage current and nonuniform charge collection. Hence the changes in the leakage current and energy resolution should occur together; this is substantiated by the data shown in figure 11.

(c) They can cause reduction in the carrier lifetime. This will lead to carrier loss through trapping and consequently reduced pulse height and energy resolution as evidenced by figures 2 to 5. A convenient measure of the change in carrier lifetime can be obtained[4] by studying the collected charge as a function of the applied bias. Figures 9 and 10 show evidence of increased carrier collection efficiency, and, hence, reduced sensitivity to damage at higher bias. This result is quite consistent with our observation of higher damage threshold for dE/dx detectors compared with normal, otherwise fully comparable, detectors.

However, there is no information available on the relative number of various types of defects and their respective carrier capture cross sections. It is therefore not possible to make an exact theoretical calculation of the proton dose of a particular energy required to produce a certain degree of degradation in a certain type of detector. Under such circumstances, it may be useful to use the experimental data to obtain an empirical relation between the observed damaging proton dose to a certain type of detector and the changes in certain performance characteristics of the detector.

[4]The proton irradiation decreases carrier lifetime τ and increases the carrier transit time T_R. In an irradiated detector, the lost charge is proportional to $\exp(-\tau/T_R)$. Now, the carrier transit time is a function of the detector bias while the carrier lifetime is determined by the condition of the detector base material. Thus, a determination of the lost charge as a function of the detector bias should permit a measurement of the change in carrier lifetime.

The radiation damage sensitivity of a detector may be expected to depend upon the following factors:

(a) Base material resistivity

(b) Detector depletion width/Range of incident protons (i.e., number of defects and their distribution)

(c) Electrical field distribution across the sensitive region of the detector

By combining all these factors, one obtains an equation of the following form:

$$\left.\begin{array}{l} \phi_X = f(\rho, V, E_O)x \\ \phi_X = f_1(\rho)f_2'(E_O, W)f_3(V, W)x \\ \phi_X = f_1(\rho)f_2(E_O, \Delta E)f_3(V, W)x \end{array}\right\} \tag{1}$$

where

ϕ_X proton dose that produces an x-fold degradation in resolving power of detector; degree of degradation   x   is defined as $\dfrac{\text{Change in resolving power}}{\text{Initial resolving power}}$

$f_1(\rho)$ function depending on initial resistivity ρ of detector base material

$f_2'(E_O, W)$ function depending on incident proton energy and the sensitive region of detector

$f_3(V, W)$ function depending on detector bias and depletion width of detector

V detector bias, volts

W depletion width of detector

$f_2(E_O, \Delta E)$ function depending on incident proton energy E_O and energy loss by proton in sensitive region of detector ΔE; ΔE is given by $\displaystyle\int_0^W \frac{dE}{dx}(E)dx = E_O - E_1$ where E_1 is energy of outgoing proton

Now the experimentally observed dependence of ϕ_X on ρ suggests that

$$f_1(\rho) \propto \exp(-\rho) = \exp(-b\rho) \tag{2}$$

where b is a constant to be determined. Similarly, the function $f_2(E_O, \Delta E)$ appears to have the following form:

$$f_2\big(E_O, \Delta E\big) \propto \big(E_O/\Delta E\big)^{1/2} = a\big(E_O/\Delta E\big)^{1/2} \tag{3}$$

9

where a is a constant to be determined. This type of dependence on $(E_0/\Delta E)$ should be valid in the case of uniform defect distribution which occurs in the following cases (see fig. 15):

(a) 20.0-MeV protons incident on 100-micron-deep, 500-micron-deep, and 500-micron-deep (dE/dx) detectors

(b) 40.0-MeV protons incident on 100-micron-deep, 500-micron-deep, and 500-micron-deep (dE/dx) detectors

For 5.0-MeV protons incident on 100-micron-deep detectors, the defect concentration rises sharply as the exit window of the detector is approached. But when 5.0 MeV protons strike a 500-micron-deep detector, all the defects are confined to the first 220 microns (most of them in the region 200 to 220 microns). Therefore, only data at 20.0 MeV and 40.0 MeV can be used to obtain b, though the 5.0-MeV data on 100-micron-deep detectors may be usable.

For normal detectors, $f_3(V,W)$ may be treated as a constant since the initial applied detector bias, in all cases, ensured complete charge collection. For dE/dx detectors, $f_3(V,W)$ will have a different value and should be treated separately. In the treatment that follows, $f_3(V,W)$ has really been incorporated in $f_2(E_0,\Delta E)$ through an appropriate value of a corresponding to $f_3(V,W)$ = Constant.

Equations (1) may now be written in the form:

$$\phi_X = ax\left[\left(E_0/\Delta E\right)^{1/2}\right]e^{-b\rho} \tag{4}$$

It should be mentioned that equation (4) has been developed on the basis of conditions stated earlier and the establishment of exact forms of $f_1(\rho)$ and $f_2(E_0,\Delta E)$ requires considerably more experimental data.

A least-square fit of the experimentally observed values of $\phi_{X=1}$ (i.e., the proton dose required to lower the resolving power of the detector by a factor of 2) to an expression of the form given by equation (4) (fig. 16) leads to the following values of a and b:

E, MeV	Detector depth, microns	$\left(E_0/\Delta E\right)^{1/2}$	a (*)	b (*)
20.0	100	6.48	$(2.61 \pm 0.26)10^{10}$	$(9.33 \pm 0.93)10^{-5}$
	500	2.90	$(4.23 \pm 0.42)10^{10}$	$(6.40 \pm 0.64)10^{-5}$
	500 (dE/dx)	2.90	$(6.14 \pm 0.61)10^{10}$	$(4.02 \pm 0.40)10^{-5}$
40.0	100	12.65	$(2.03 \pm 0.20)10^{10}$	$(5.52 \pm 0.55)10^{-5}$
	500	5.65	$(2.89 \pm 0.29)10^{10}$	$(7.96 \pm 0.80)10^{-5}$
	500 (dE/dx)	5.65	$(4.16 \pm 0.41)10^{10}$	$(4.02 \pm 0.40)10^{-5}$

*The errors on the values of a and b are either least-square values or 10 percent of the mean value, whichever is greater.

For proton energies and detector depths which ensure uniform defect distribution, the following forms of equation (4) are obtained for $x = 1$:

Normal detectors:

$$\phi_{x=1} = (2.94 \pm 1.20)10^{10}\left(E_0/\Delta E\right)^{1/2} \exp\left(\overline{-7.30 \pm 2.30} \times 10^{-5}\,\rho\right) \tag{5}$$

dE/dx detectors:

$$\phi_{x=1} = (5.10 \bullet 1.00)10^{10}\left(E_0/\Delta E\right)^{1/2} \exp\left(\overline{-4.00 \pm 0.50} \times 10^{-5}\,\rho\right) \tag{6}$$

The difference in the values of a for the normal detectors and the dE/dx type detectors reflects the fact that $f_3(V,W)$ has different values for these two types of detectors. The difference in the values of b, however, is slightly puzzling at first sight. It is perhaps attributable to the role played by the electrical field on the defect distribution. The reduced value of b implies an effectively smaller value of ρ or reduced efficiency of the defects for carrier removal. Figure 17 shows a comparison of the calculated values of $\phi_{x=1}/(E/\Delta E)^{1/2}$ with the experimental values for both types of detectors.

If the entire proton energy had been used up in defect production – or the same fraction thereof at 20.0 MeV and 40.0 MeV – the ratios of the equivalent damage doses would be expected to be as indicated in table IV. The experimentally observed values of the ratios of the equivalent proton doses for detectors of different thicknesses tend to reflect the effects of low fields in thicker detectors.

CONCLUDING REMARKS

The detectors made from lower resistivity base materials show considerably greater resistance to damage than those made from higher resistivity materials. The use of larger collecting fields across the sensitive region also increases the radiation resistance of the detectors. Among the normal detectors tested in this investigation, those made from base materials with resistivity in the range 5 to 10 kΩ-cm did not show any signs of damage up to dose levels of the order of 3×10^9 to 5×10^9 protons/cm^2 in the case of protons stopped in the detectors. The damage sensitivity, as expected, is lower at higher proton energies. In the case of dE/dx detectors, there was no convincing evidence of any difference in degradation rates when viewed from the positive or negative sides of the detectors. The damage threshold of dE/dx detectors is higher than that of comparable normal detectors. The junction capacitance does go down with the proton dose though not as fast as one might anticipate on the basis of variation in the base material resistivity.

The phenomenological expressions developed in this report predict typical twofold doses and may be used in the absence of specific data. However, it must be borne in mind that significant excursions from the mean values predicted by these expressions can occur.

Langley Research Center,
National Aeronautics and Space Administration,
Langley Station, Hampton, Va., November 20, 1967,
125-24-03-21-23.

REFERENCES

1. Goulding, F. S.: Semiconductor Detectors for Nuclear Spectrometry, I. Nucl. Instr. Methods, vol. 43, no. 1, Aug. 1, 1966, pp. 1-54.

2. Tove, P. A.; and Falk, K.: Transit Time of Charge Carriers in the Semiconductor Ionization Chamber. Nucl. Instr. Methods, vol. 12, no. 2, July 1961, pp. 278-290.

3. Eisler, P.: Inefficient Charge Collection in Silicon Surface Barrier Detectors. Nucl. Instr. Methods, vol. 44, no. 2, Oct. 1966, pp. 253-260.

4. Dabbs, J. W. T.; and Walter, F. J., eds.: Semiconductor Nuclear Particle Detectors. Publ. 871, Natl. Acad. Sci.—Natl. Res. Council, 1961.

5. Dearnaley, G.; and Northrop, D. C.: Semiconductor Counters for Nuclear Radiations. Second ed., E. & F. N. Spon Ltd. (London), 1966.

6. George, G. G.; and Gunnersen, E. M.: Irradiation Damage Effects in Silicon Surface Barrier Counters. Nucl. Instr. Methods, vol. 25, no. 2, Jan. 1964, pp. 253-260.

7. Dearnaley, G.; and Whitehead, A. B.: The Semiconductor Surface Barrier for Nuclear Particle Detection. Nucl. Instr. Methods, vol. 12, no. 2, July 1961, pp. 205-226.

8. Halbert, M. L.: Surface-Barrier Counters for Nuclear Reaction Studies. Nuclear Electronics – I, Intern. At. Energy Agency (Vienna), 1962, pp. 403-413.

TABLE I.- EFFECT OF 5.0-MeV-PROTON IRRADIATION ON THE DECTORS

No.	Detector type	Detector bias, V	Base material resistivity, kΩ-cm	Base material carrier lifetime, μsec	Proton dose at which first signs of damage occur, protons/cm^2 (a)	Proton dose for twofold increase in Po^{210} peak width, protons/cm^2
			Source A detectors			
1	100 μ, normal	30	1.9	100 to 500	6.8×10^9	2.49×10^{10}
2	500 μ, normal	130	10.5	1250 to 1350	4.5×10^9	3.1×10^{10}
3	500 μ, dE/dx	220	10.5	1250 to 1350	8.0×10^9	6.0×10^{10}
			Source B detectors			
1	100 μ, normal	60	1.0	400	4.5×10^9	3.74×10^{10}
2	500 μ, normal	200	5.0	1500	4.0×10^9	4.9×10^{10}
3	500 μ, dE/dx	120	9.5	3000	6.5×10^9	5.6×10^{10}
			Source C detectors			
1	100 μ, normal	30	5.9 to 7.2	500 to 600	3.1×10^9	2.0×10^{10}
2	500 μ, dE/dx	150	5.9 to 7.2	500 to 600	1.0×10^{10}	8.0×10^{10}
			Source D detectors			
1	100 μ, normal	8	28	1000	4.5×10^8	5.0×10^9
2	500 μ, normal	100	10 to 12	1000	4.0×10^{10}	4.0×10^{10}
3	500 μ, dE/dx	50	22	1000	4.6×10^{10}	4.6×10^{10}

[a]Significant damage is considered to have occurred when the Po^{210} alpha resolution has deteriorated by 10 percent.

TABLE II.- EFFECT OF 20.0-MeV-PROTON IRRADIATION ON THE DETECTORS

No.	Detector type	Detector bias, V	Base material resistivity, $k\Omega$-cm	Base material carrier lifetime, μsec	Proton dose at which first signs of damage occur, protons/cm^2 (a)	Proton dose for twofold increase in Po^{210} peak width, protons/cm^2
			Source A detectors			
1	100 μ, normal	30	1.9	100 to 500	4.5×10^{10}	1.35×10^{11}
2	500 μ, normal	110	10.2	1250 to 1350	8.0×10^{9}	5.0×10^{10}
3	500 μ, dE/dx	120	10.2	1250 to 1350	2.5×10^{10}	11.0×10^{10}
			Source B detectors			
1	100 μ, normal	50	1.0	400	3.5×10^{10}	1.55×10^{11}
2	500 μ, normal	200	4.8	1500	1.1×10^{10}	1.0×10^{11}
3	500 μ, dE/dx	300	20	5000	8.0×10^{9}	8.0×10^{10}
			Source C detectors			
1	100 μ, normal	20	5.9 to 7.2	500 to 600	2.2×10^{10}	9.0×10^{10}
2	500 μ, normal	150	5.9 to 7.2	500 to 600	1.0×10^{10}	9.0×10^{10}
3	500 μ, dE/dx	15	5.9 to 7.2	500 to 600	3.0×10^{10}	14.0×10^{10}
			Source D detectors			
1	100 μ, normal	8	28	1000	3.0×10^{9}	1.3×10^{10}
2	500 μ, normal	100	22	1000	4.0×10^{9}	3.3×10^{10}
3	500 μ, dE/dx	100	10 to 12	1000	3.0×10^{10}	1.2×10^{11}

[a]Significant damage is considered to have occurred when the Po^{210} alpha resolution has deteriorated by 10 percent.

TABLE III.- EFFECT OF 40.0-MeV-PROTON IRRADIATION ON THE DETECTORS

No.	Detector type	Detector bias, V	Base material resistivity, $k\Omega$-cm	Base material carrier lifetime, μsec	Proton dose at which first signs of damage occur, protons/cm^2 (a)	Proton dose for twofold increase in Po^{210} peak width, protons/cm^2
			Source A detectors			
1	100 μ, normal	130	1.4	100 to 500	7.1×10^{10}	2.2×10^{11}
2	500 μ, normal	110	.9	1300	9.0×10^{9}	8.0×10^{10}
			Source B detectors			
1	100 μ, normal	50	1	400	9.8×10^{10}	2.6×10^{11}
2	500 μ, normal	200	5	1500	1.5×10^{10}	1.1×10^{11}
3	500 μ, dE/dx	170	9.5	3000	4.0×10^{10}	1.6×10^{11}
			Source C detector			
1	100 μ, normal	110	6.5	550	4.2×10^{10}	1.8×10^{11}

[a]Significant damage is considered to have occurred when the Po^{210} alpha resolution has deteriorated by 10 percent.

TABLE IV.- RATIOS OF THE EQUIVALENT PROTON DOSES FOR
TWOFOLD DEGRADATION AT 20.0 MeV AND 40.0 MeV

Detector thickness, microns	$\dfrac{\left(\Delta E_p\right) 20 \text{ MeV}}{\left(\Delta E_p\right) 40 \text{ MeV}}$ (Theoretical)	$\dfrac{\phi_{x=1} \text{ at 40 MeV}}{\phi_{x=1} \text{ at 20 MeV}}$ (Experimental)
100	1.79	1.75 ⎫
500	1.79	1.22 ⎬ ±25%
500 (dE/dx)	1.79	1.42 ⎭
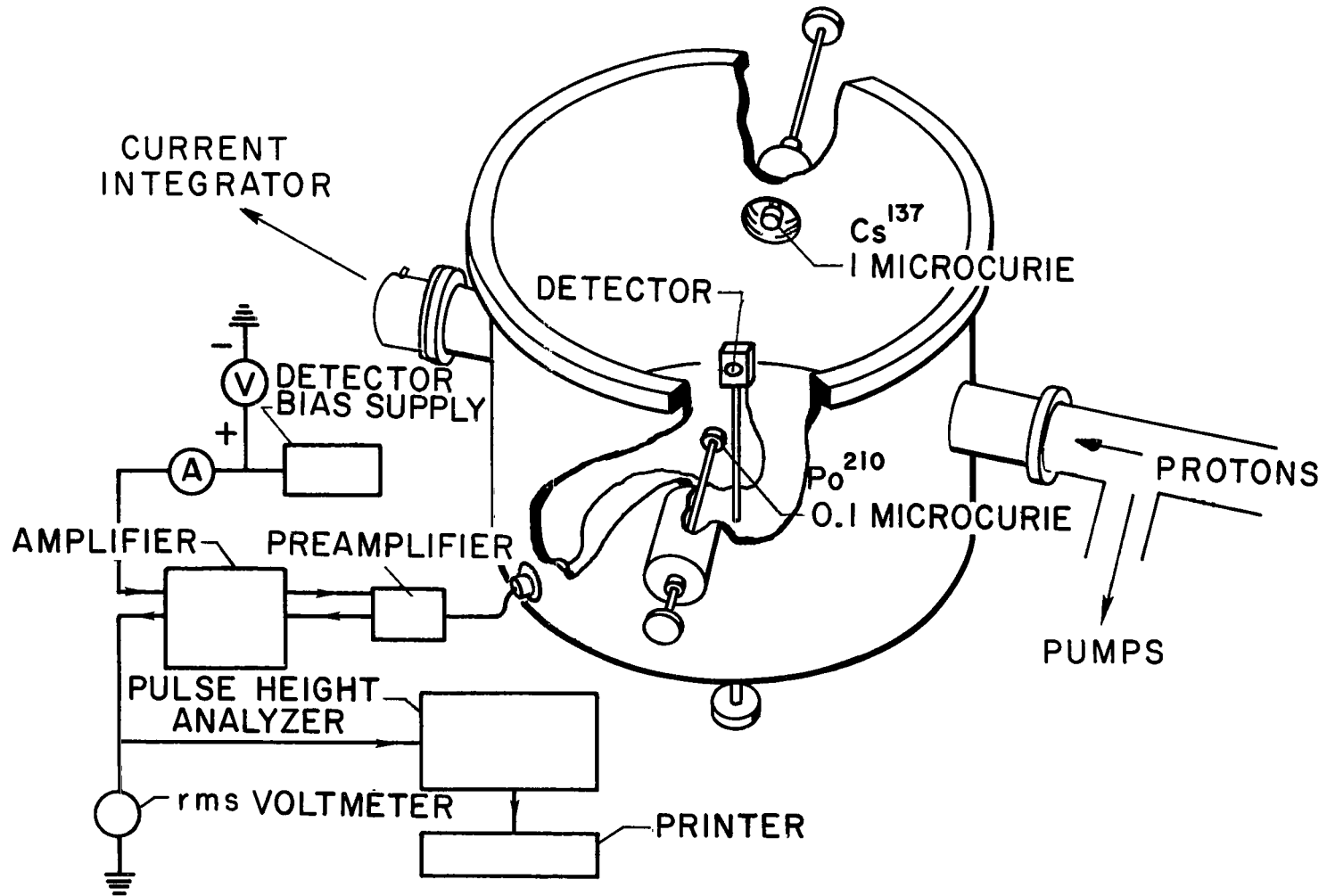
Figure 1.- Schematic diagram of the general experimental technique.
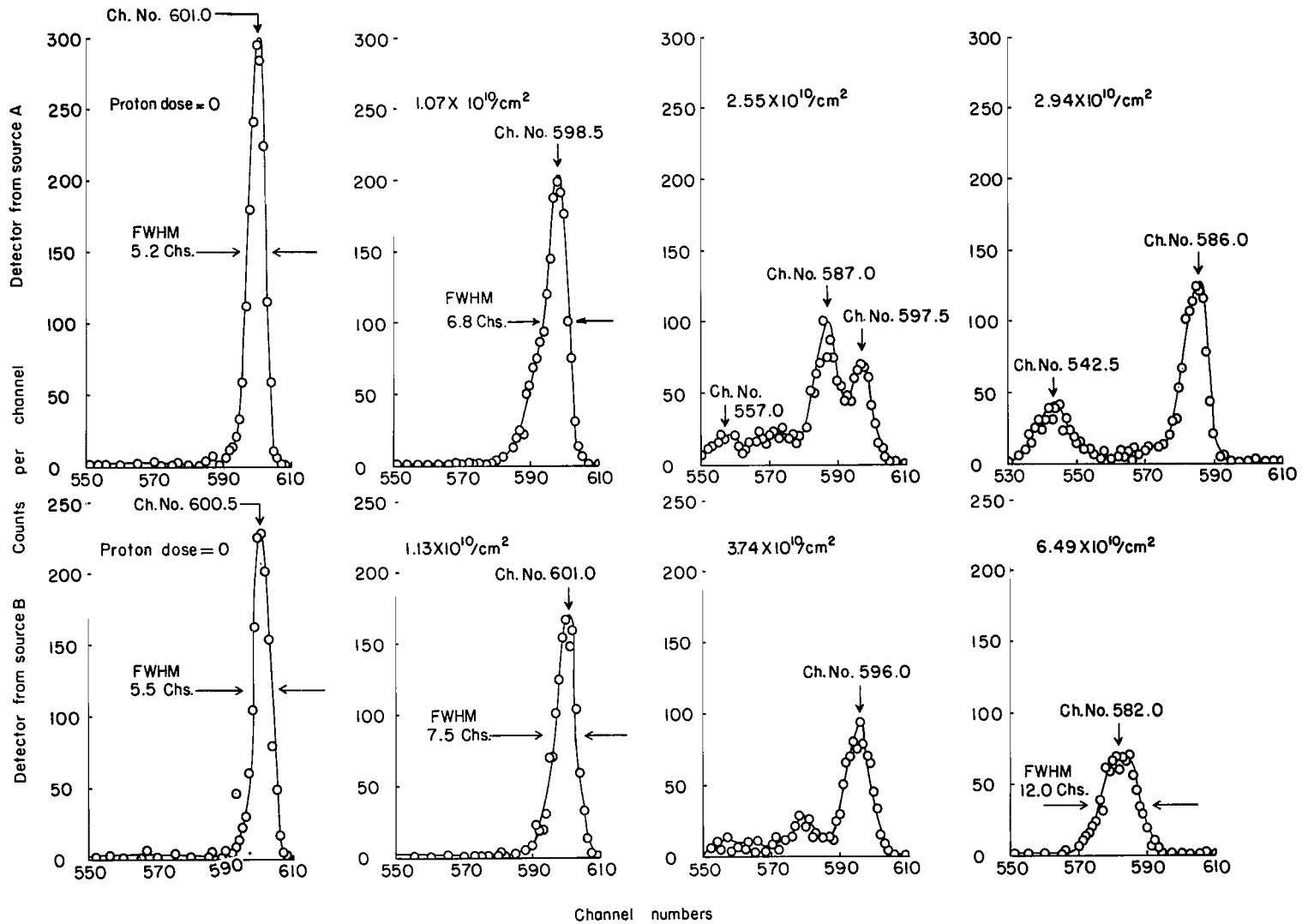
Figure 2.- Effect of 5.0-MeV proton dose on the pulse height and pulse width of the Po^{210} alpha pulses from two 100-micron-deep detectors from two different sources.
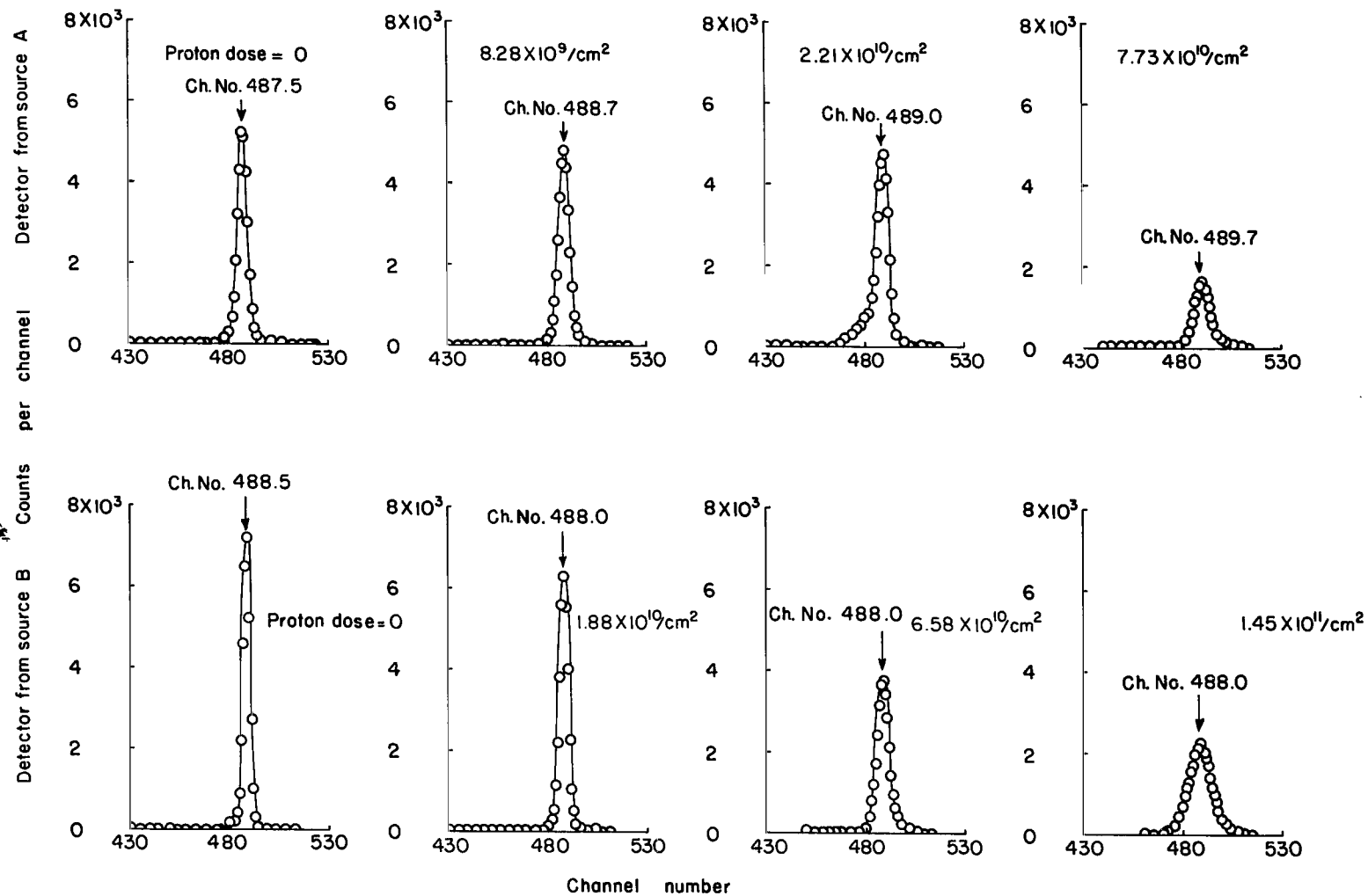
Figure 3.- Effect of 40.0-MeV proton dose on the pulse height and pulse width of Po^{210} alpha pulses from two 500-micron-deep detectors from two different sources.
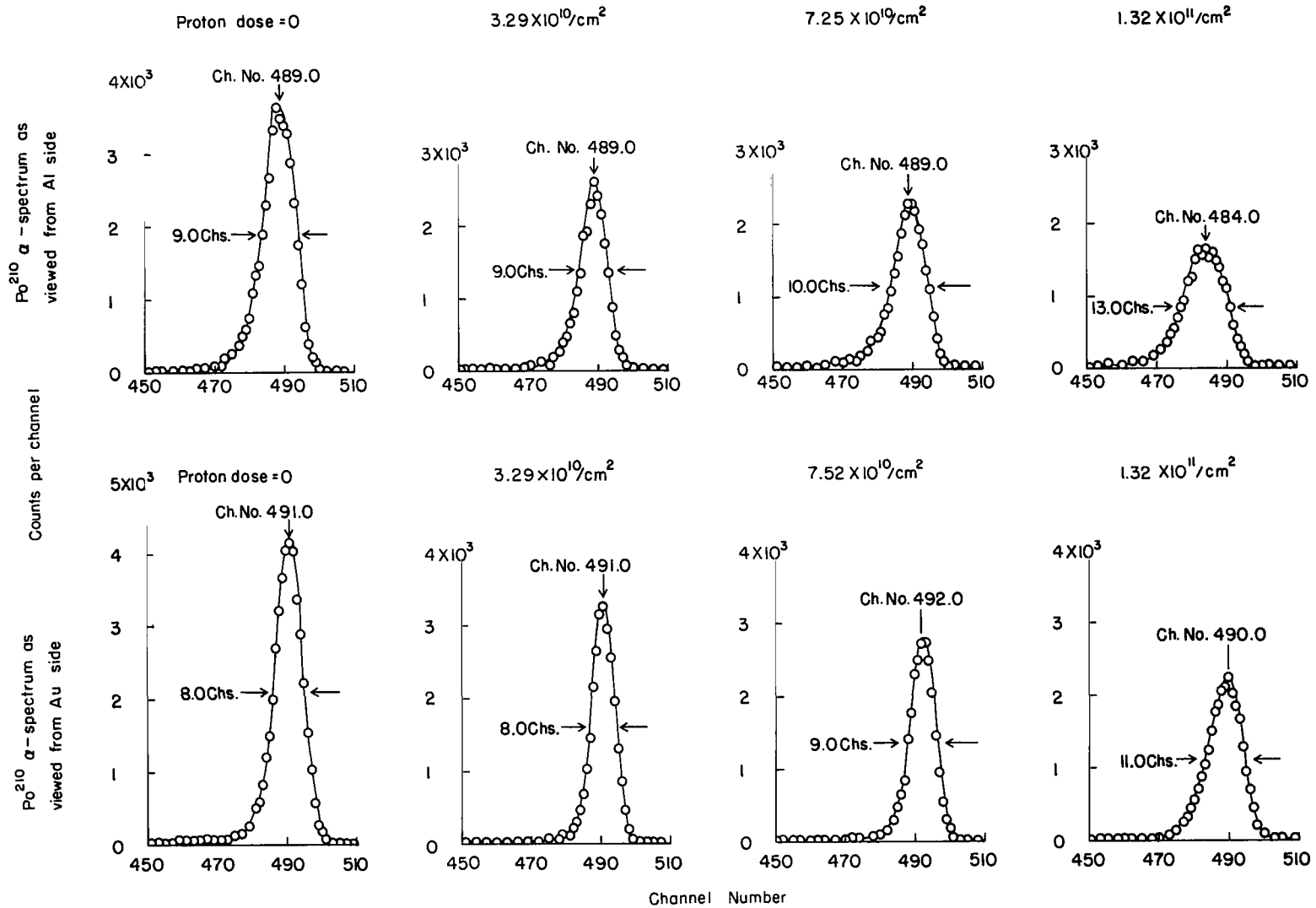
Figure 4.- Damage as a function of proton dose at 40.0 MeV in a 500-micron-deep $\left(\frac{dE}{dx}\right)$ detector from source B.
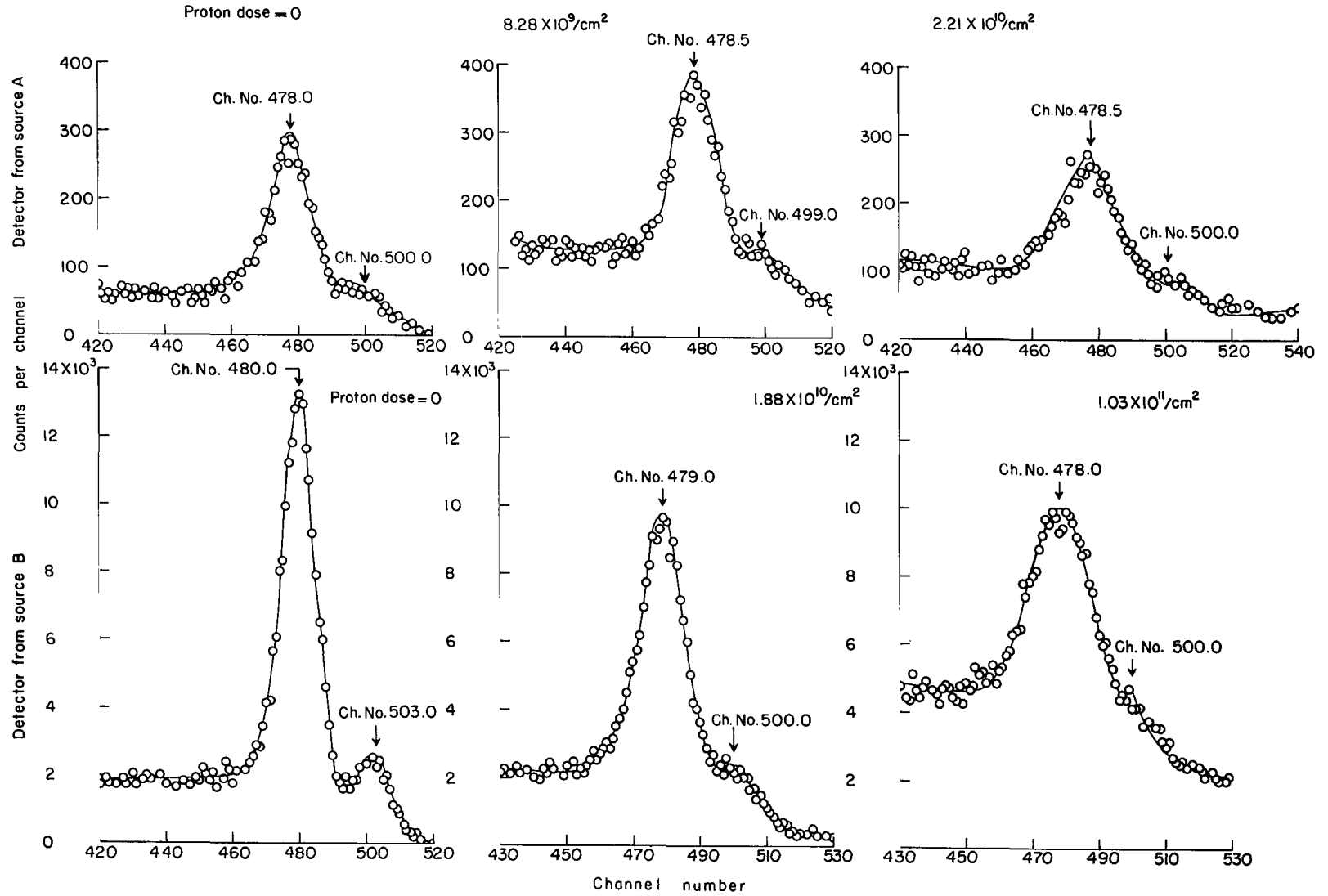
Figure 5.- The Cs^{137} electron resolution at different stages of 40.0-MeV proton damage in 500-micron-deep detectors from two different sources.
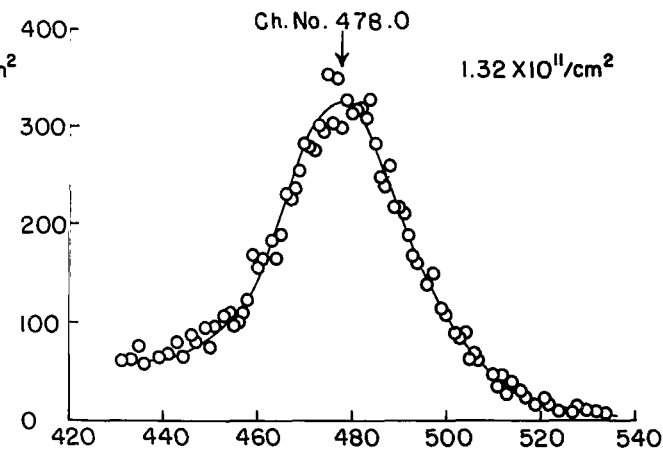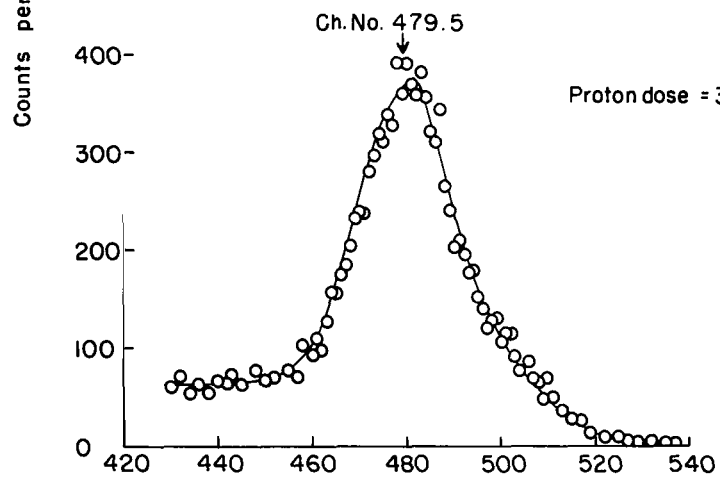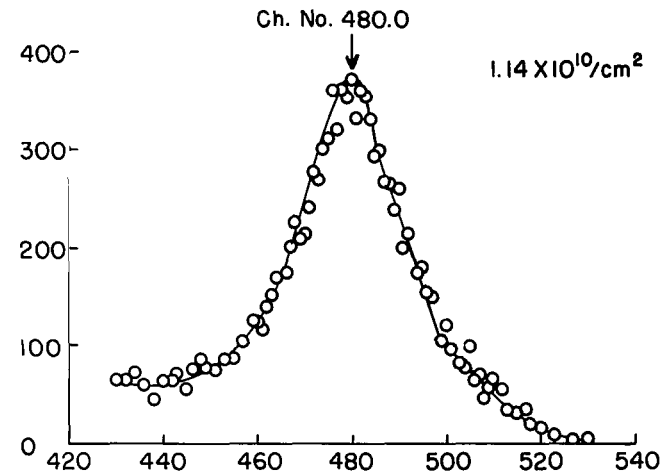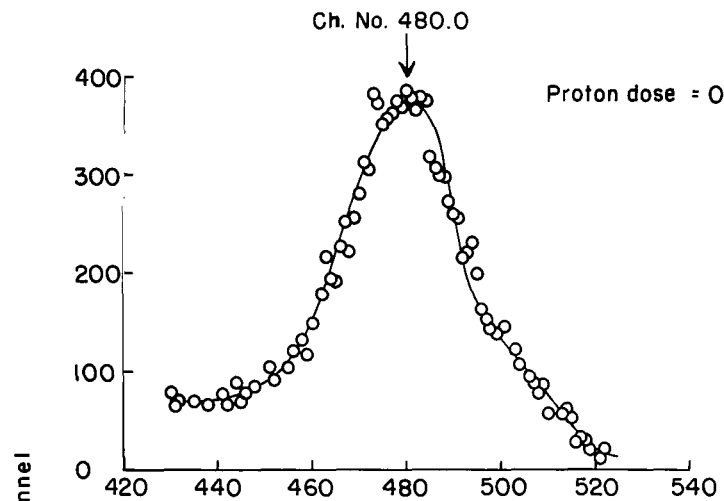
Figure 6.- Effect of 40.0-MeV proton exposure on Cs^{137} electron spectrum from a 500-micron-deep $\left(\frac{dE}{dx}\right)$ detector.
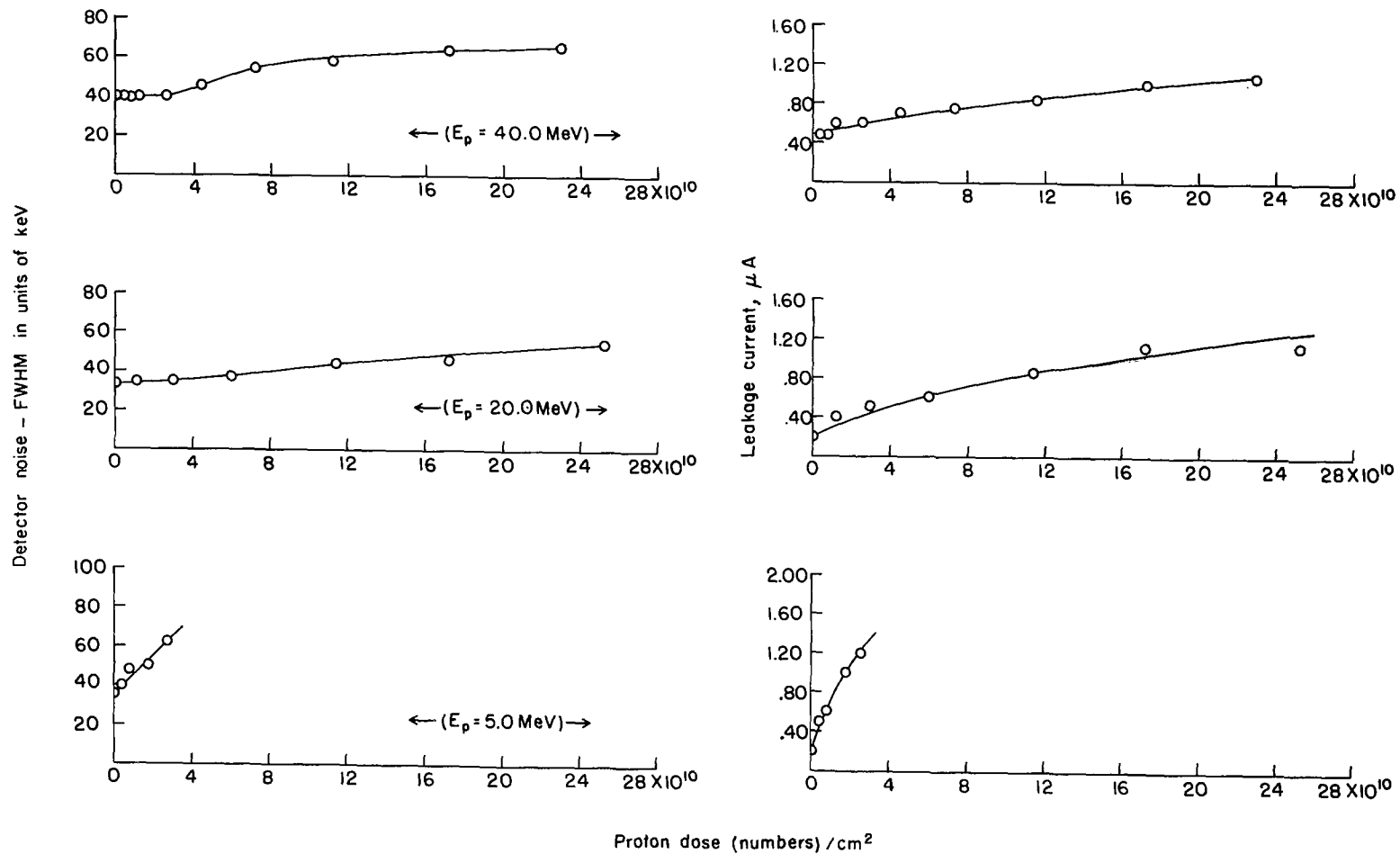
Figure 7.- Energy dependence of radiation damage in 100-micron-deep detectors.
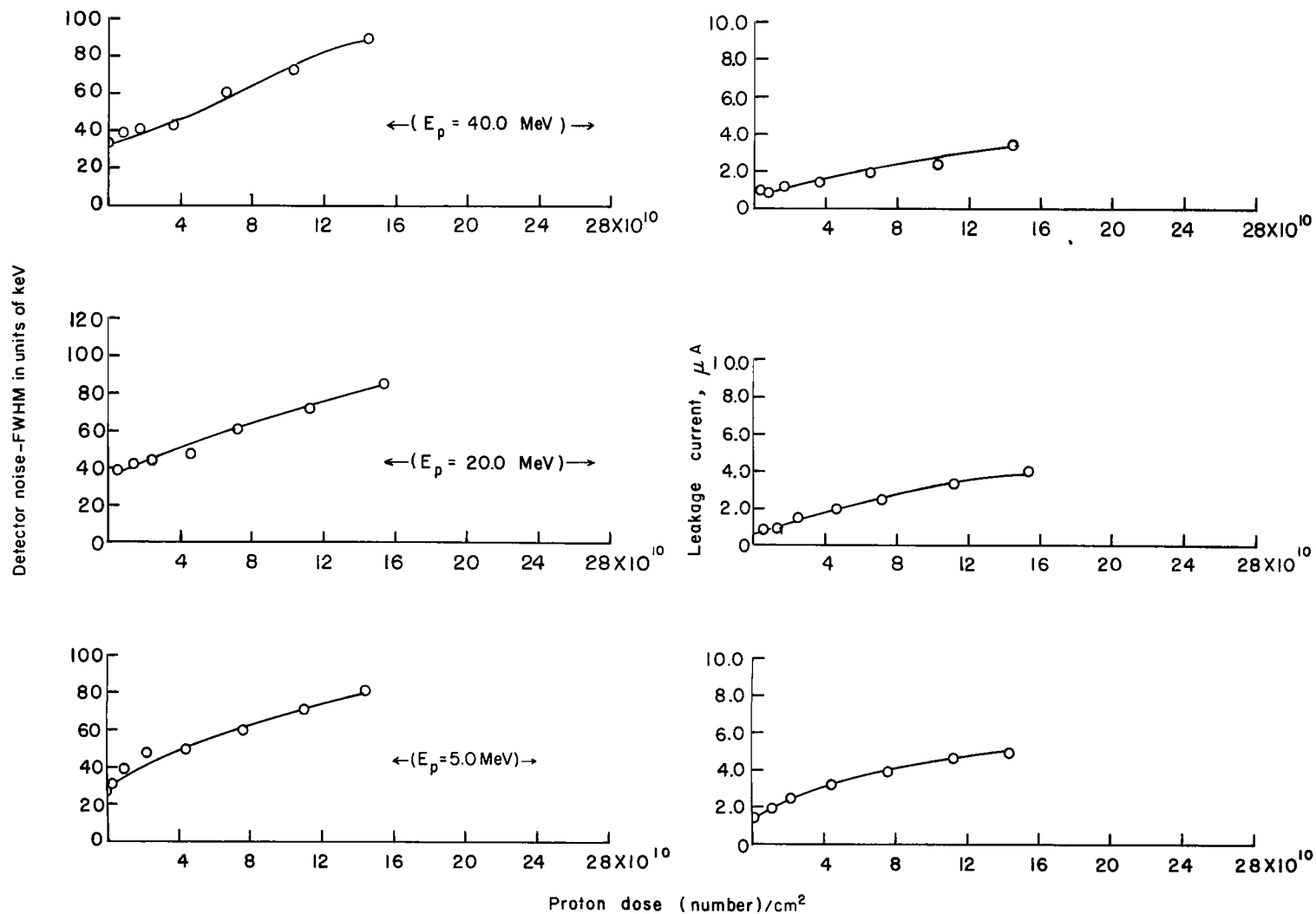
Figure 8.- Energy dependence of radiation damage in 500-micron-deep detectors.
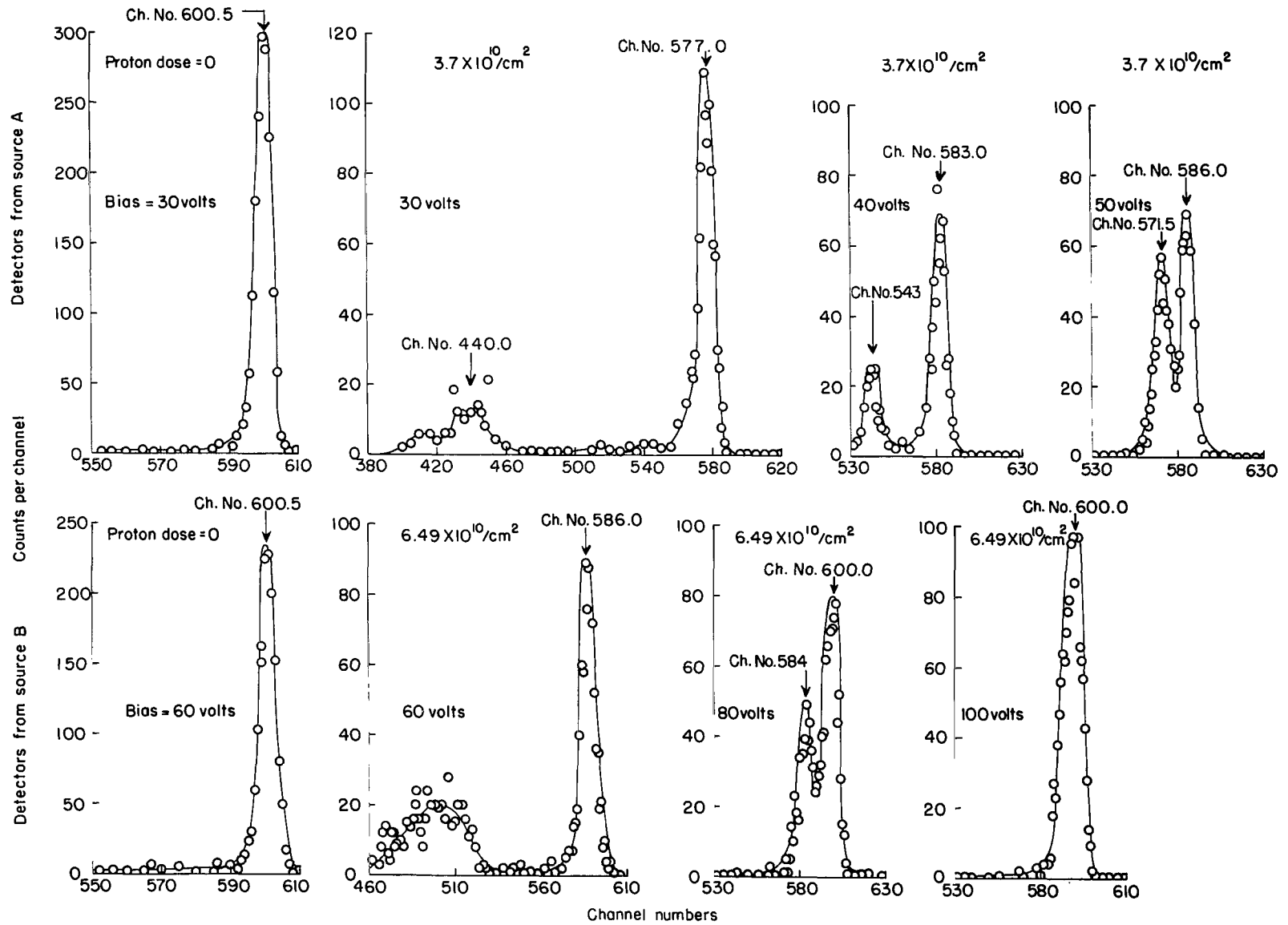
Figure 9.- Effect of increased bias on Po^{210} alpha pulses from 5.0-MeV proton damaged 100-micron-deep detectors.
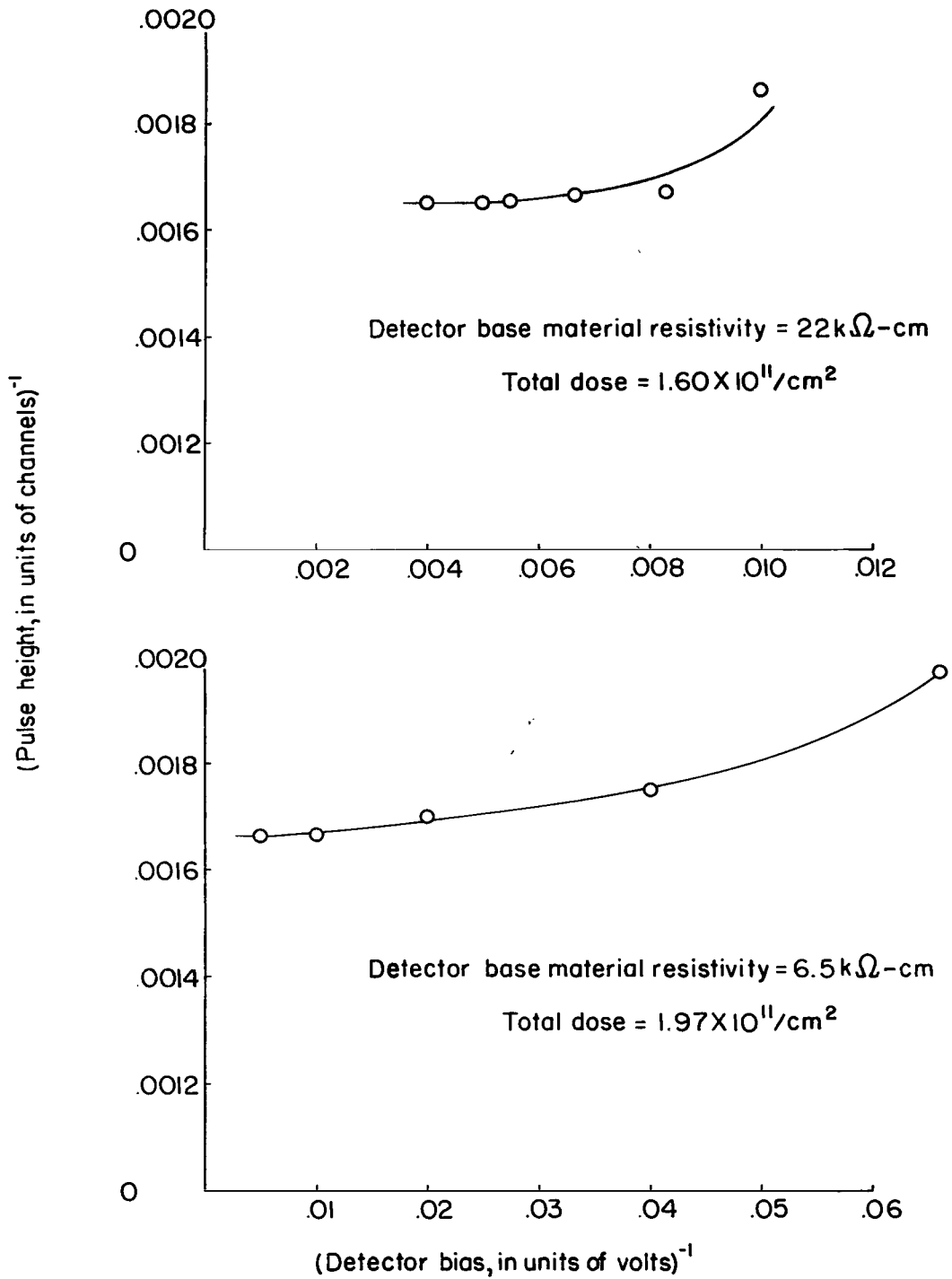
Figure 10.- Charge collection efficiency as a function of applied voltage after exposure to 20.0-MeV protons: (pulse height)$^{-1}$ plotted against (bias)$^{-1}$.
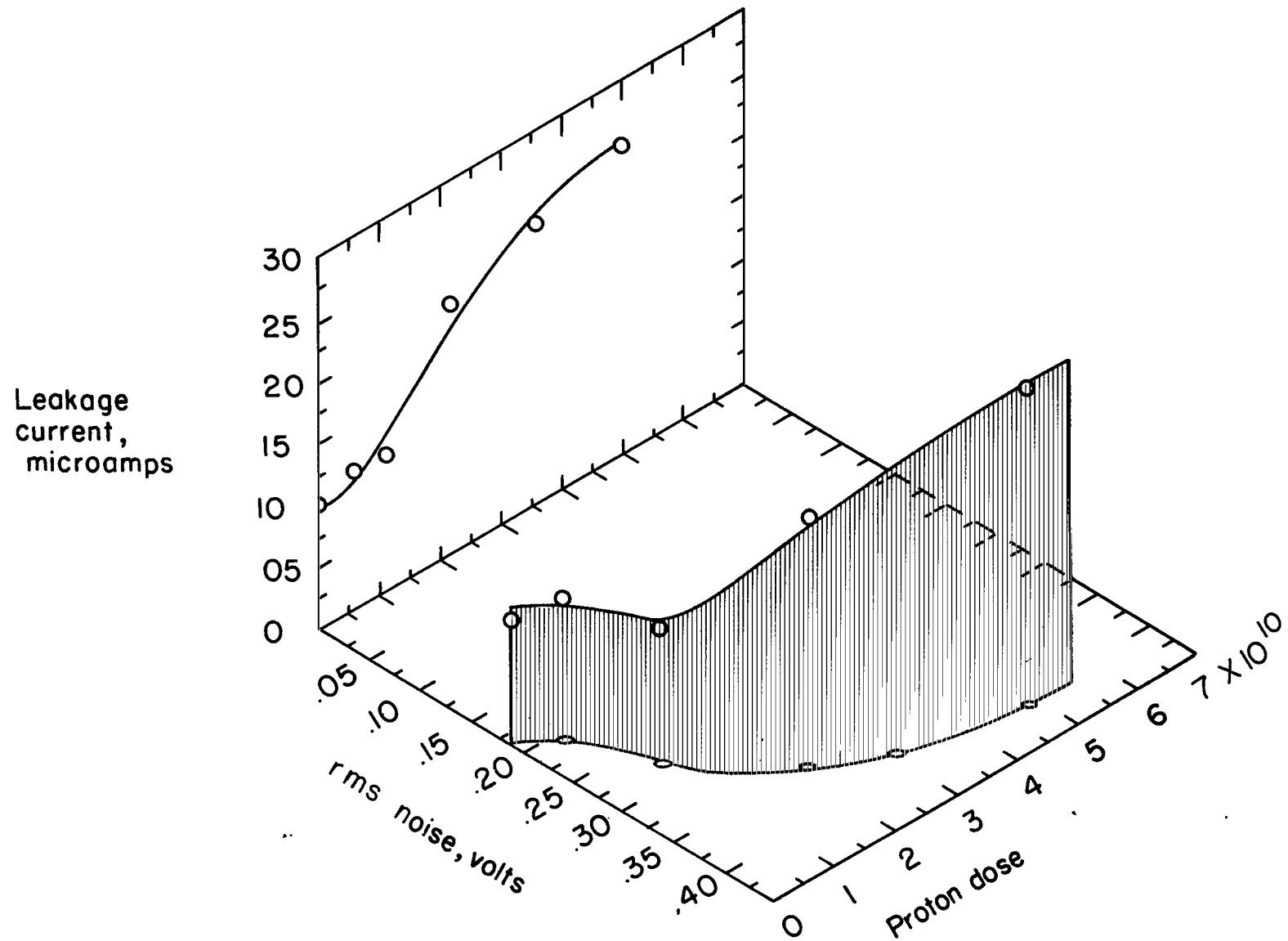
Figure 11.- Leakage current and rms noise plotted against 5.0-MeV proton dose in a 100-micron-deep detector.
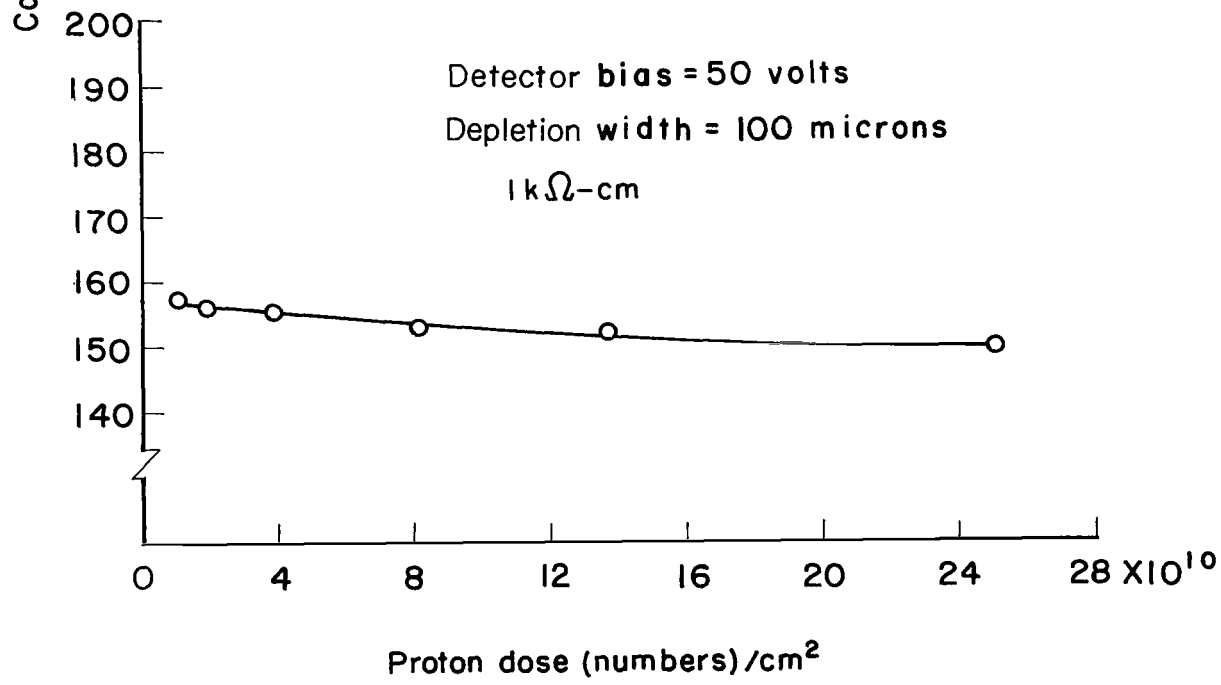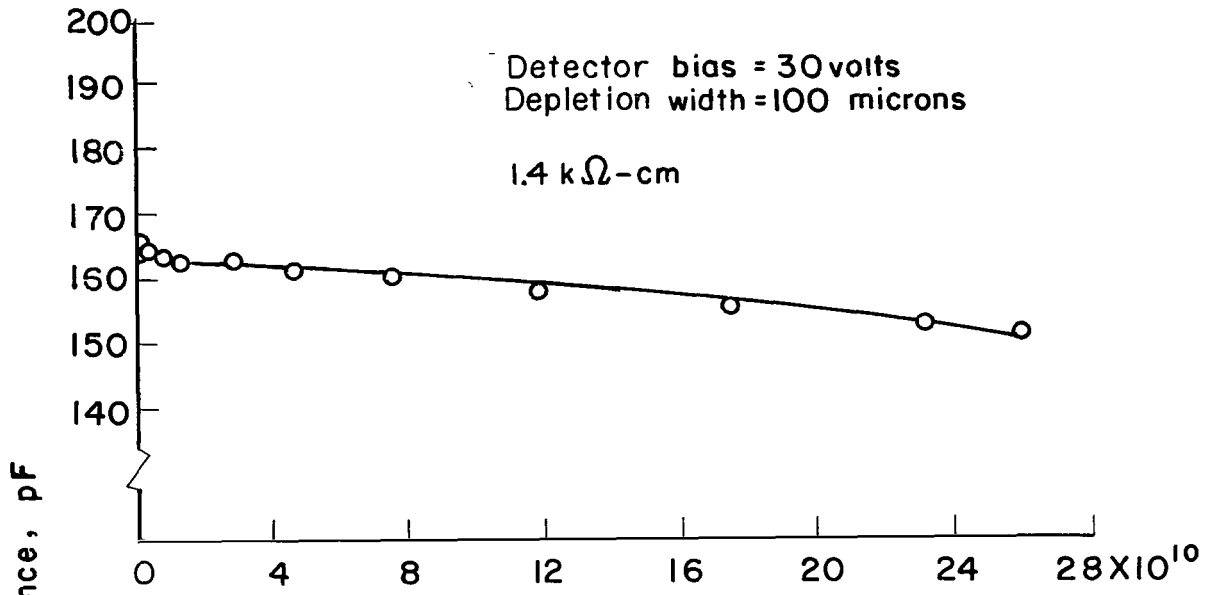
Figure 12.- Capacitance plotted against proton dose at 40.0 MeV.
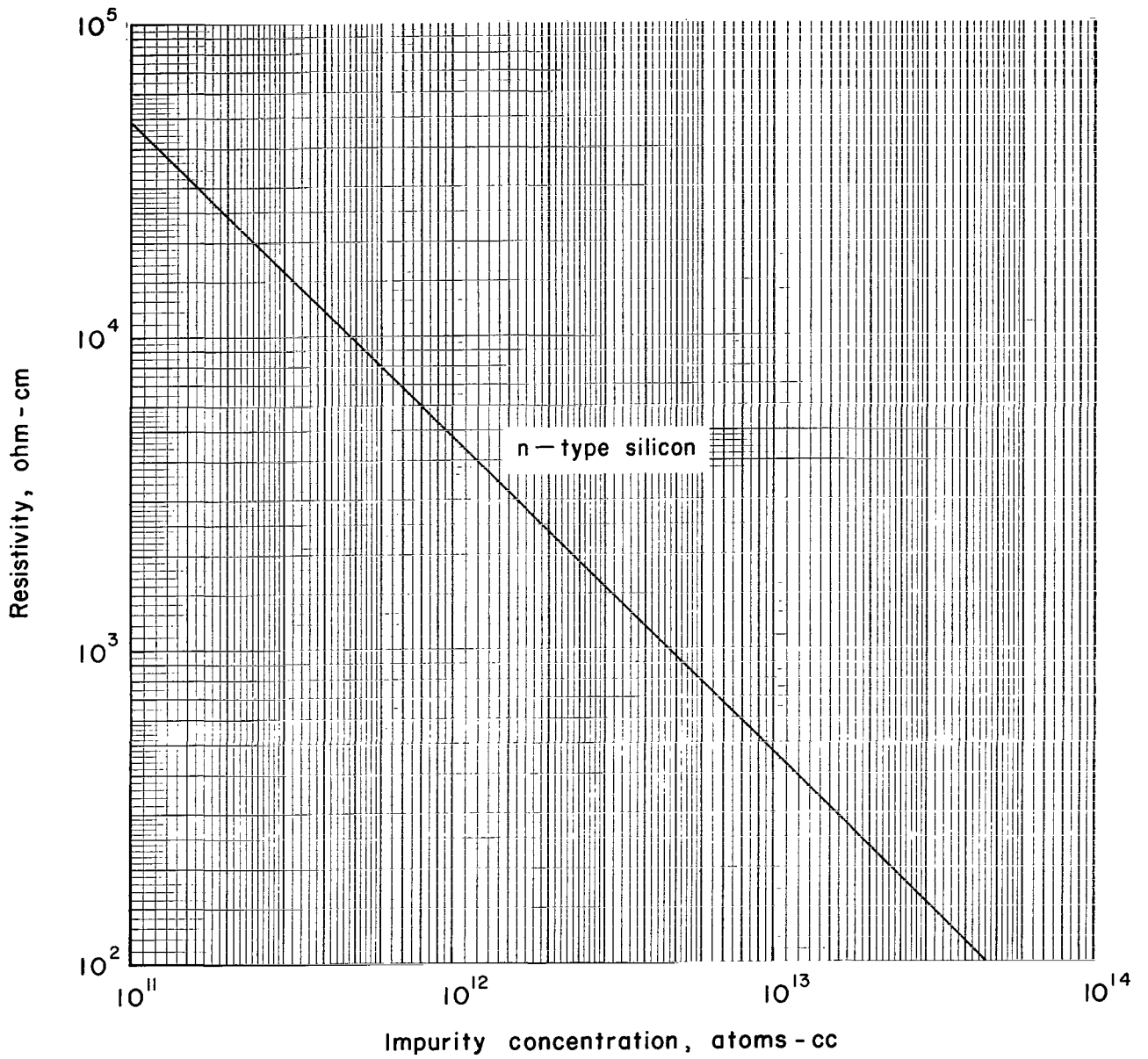
Figure 13.- Resistivity plotted against impurity concentration for silicon (ref. 5).
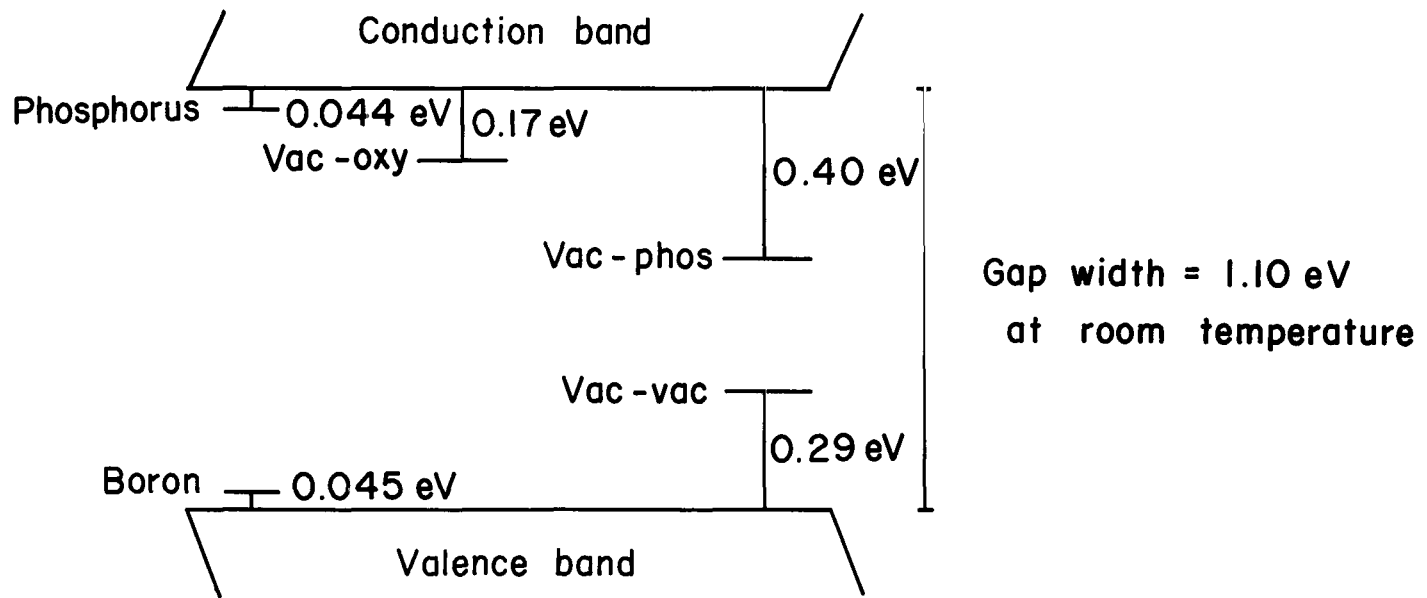
Figure 14.- Defect level scheme in irradiated silicon (ref. 4).
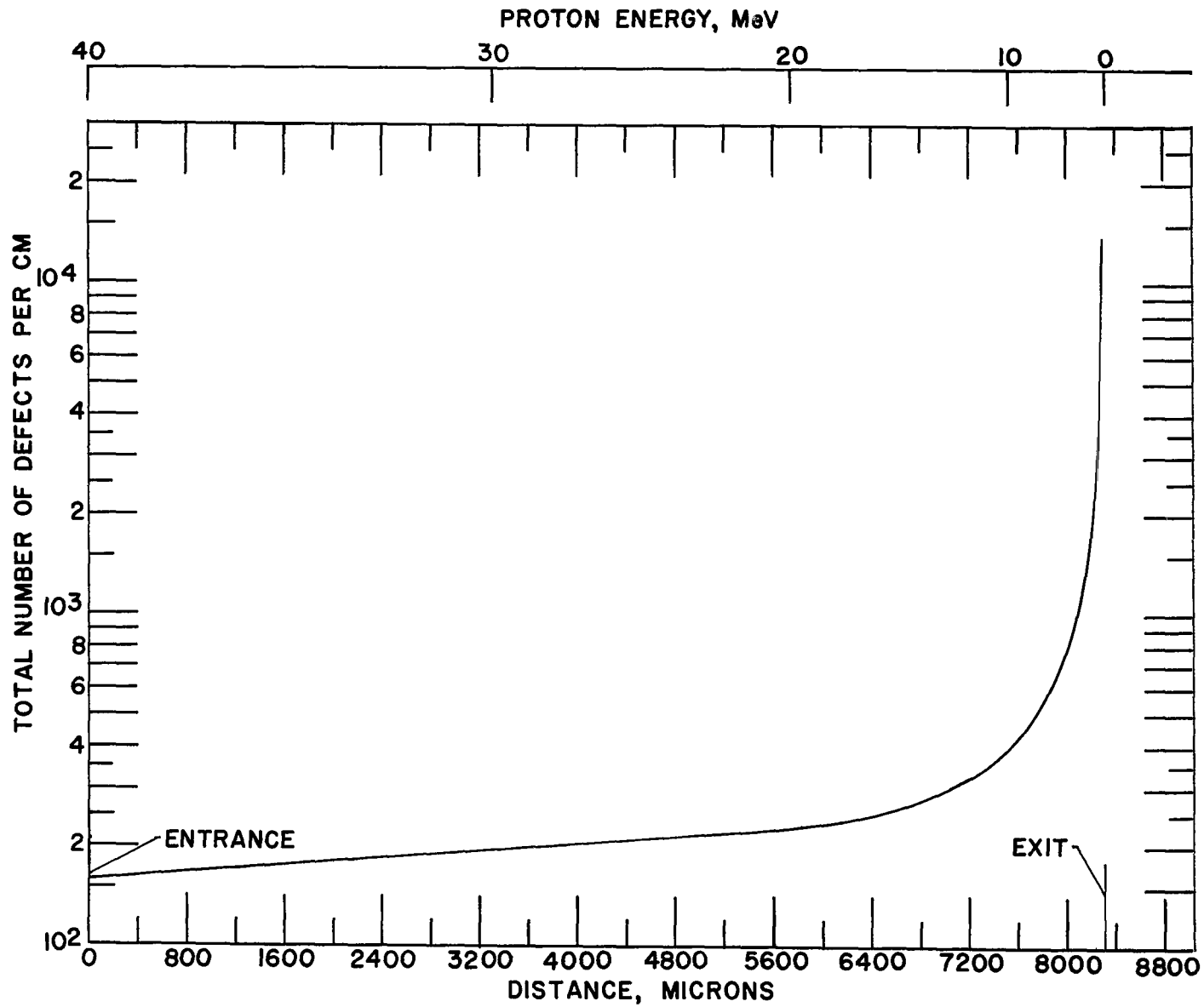
Figure 15.- Distribution of defects produced by 40-MeV protons in silicon.
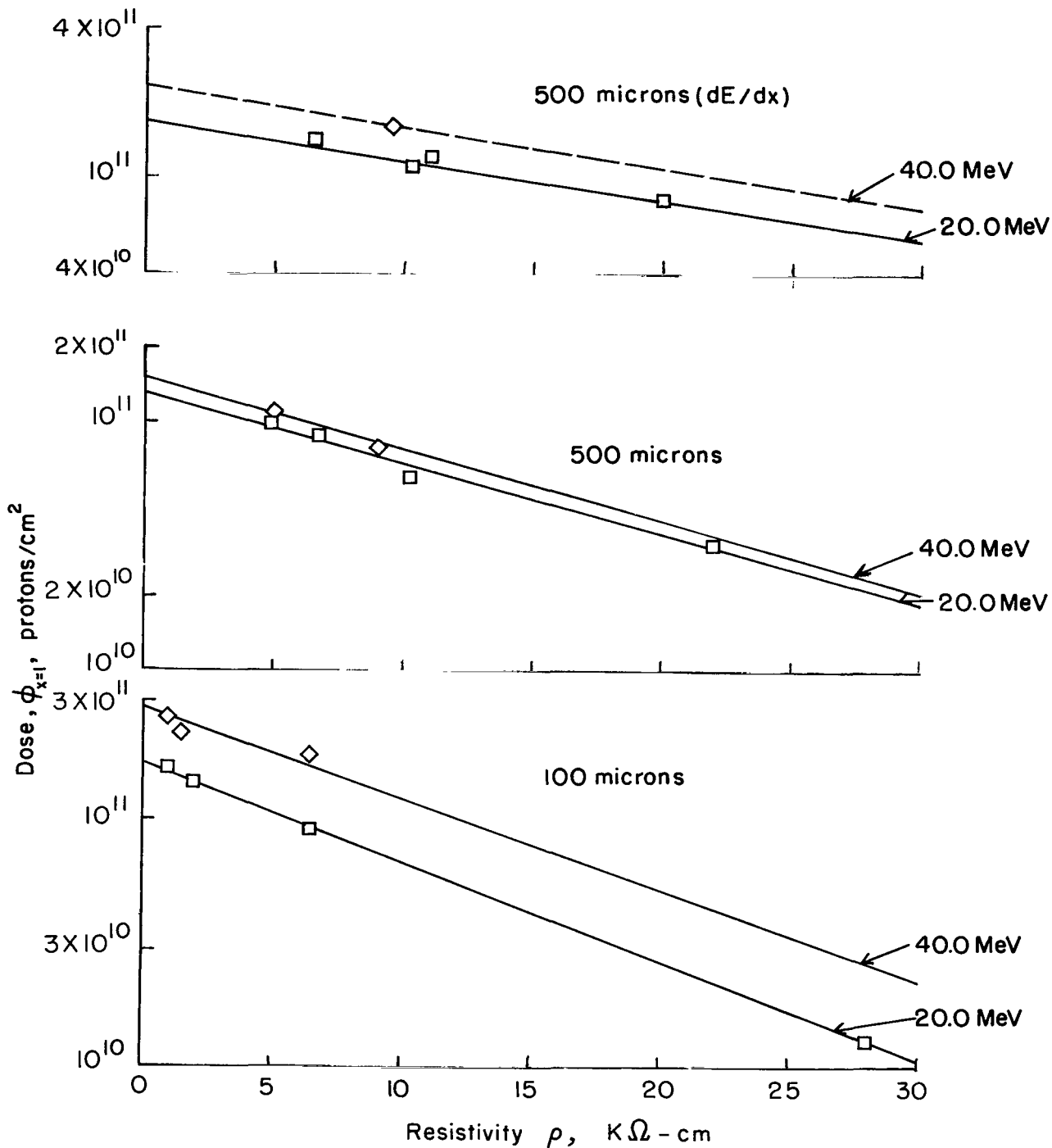
Figure 16.- Damage sensitivity of different thickness surface barrier detectors for various proton energies as a function of base material resistivity. The accuracy of resistivity and dose $(\Phi)_{x=1}$ ranges from 10 to 20 percent.
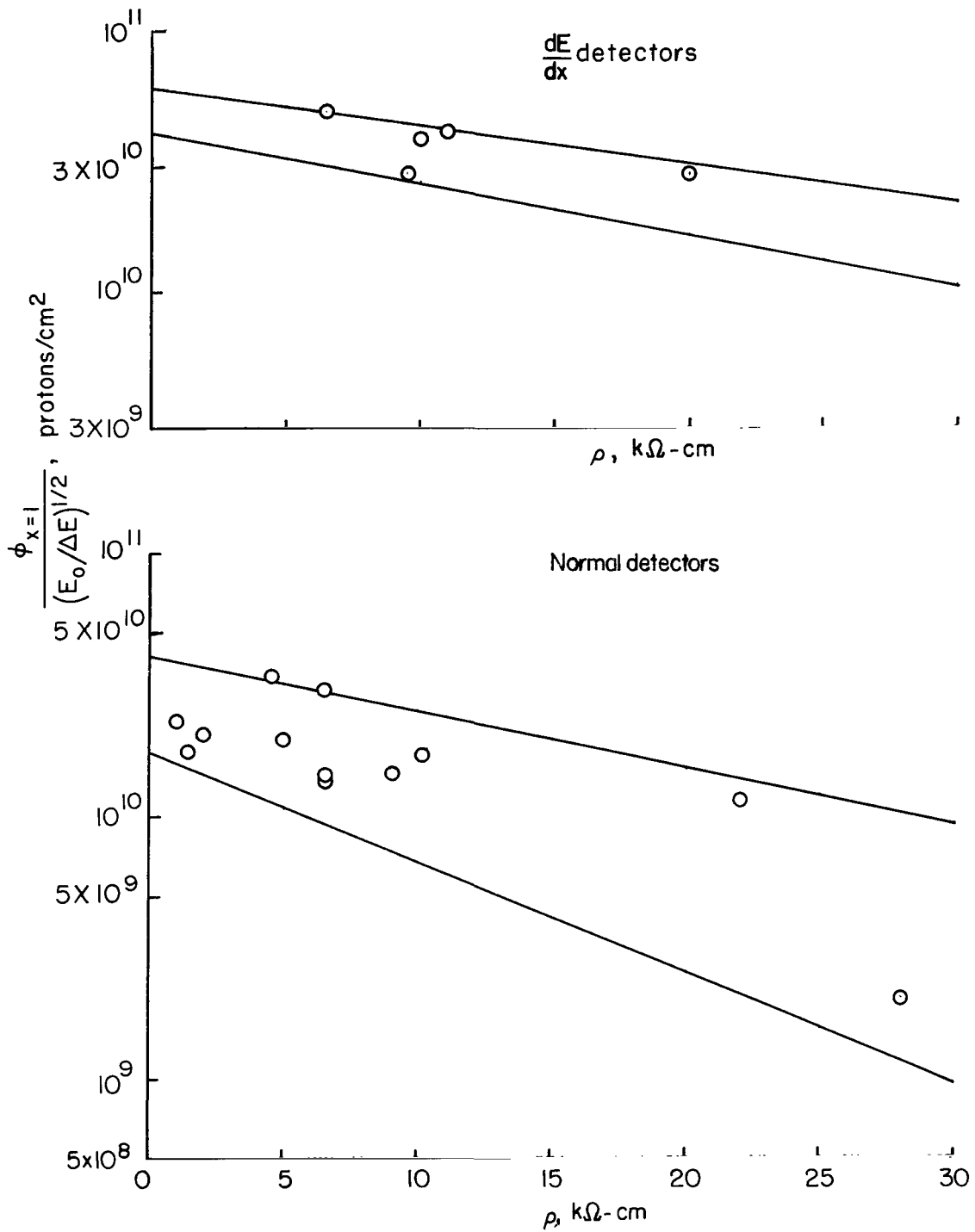
Figure 17.- Comparison of the calculated values of $\Phi_{x=1}/(E_0/\Delta E)^{1/2}$ with the experimental results. Solid lines indicate limits of predicted values.

FIRST CLASS MAIL

"The aeronautical and space activities of the United States shall be conducted so as to contribute . . . to the expansion of human knowledge of phenomena in the atmosphere and space. The Administration shall provide for the widest practicable and appropriate dissemination of information concerning its activities and the results thereof."

— NATIONAL AERONAUTICS AND SPACE ACT OF 1958

NASA SCIENTIFIC AND TECHNICAL PUBLICATIONS

TECHNICAL REPORTS: Scientific and technical information considered important, complete, and a lasting contribution to existing knowledge.

TECHNICAL NOTES: Information less broad in scope but nevertheless of importance as a contribution to existing knowledge.

TECHNICAL MEMORANDUMS: Information receiving limited distribution because of preliminary data, security classification, or other reasons.

CONTRACTOR REPORTS: Scientific and technical information generated under a NASA contract or grant and considered an important contribution to existing knowledge.

TECHNICAL TRANSLATIONS: Information published in a foreign language considered to merit NASA distribution in English.

SPECIAL PUBLICATIONS: Information derived from or of value to NASA activities. Publications include conference proceedings, monographs, data compilations, handbooks, sourcebooks, and special bibliographies.

TECHNOLOGY UTILIZATION PUBLICATIONS: Information on technology used by NASA that may be of particular interest in commercial and other non-aerospace applications. Publications include Tech Briefs, Technology Utilization Reports and Notes, and Technology Surveys.

Details on the availability of these publications may be obtained from:

SCIENTIFIC AND TECHNICAL INFORMATION DIVISION

NATIONAL AERONAUTICS AND SPACE ADMINISTRATION

Washington, D.C. 20546